Role of Vibrational and Translational Energy in the OH + NH3 Reaction: A Quasi-Classical Trajectory Study

ARTICLE *in* THE JOURNAL OF PHYSICAL CHEMISTRY A · JUNE 2013

Impact Factor: 2.69 · DOI: 10.1021/jp403571y

2 AUTHORS:

Manuel Monge-Palacios
University of Missouri
21 PUBLICATIONS **70** CITATIONS

SEE PROFILE

Joaquin Espinosa-Garcia
Universidad de Extremadura
141 PUBLICATIONS **2,171** CITATIONS

SEE PROFILE

THE JOURNAL OF PHYSICAL CHEMISTRY A

Article

pubs.acs.org/JPCA

Role of Vibrational and Translational Energy in the OH + NH_3 Reaction: A Quasi-Classical Trajectory Study

M. Monge-Palacios and J. Espinosa-Garcia*

Departamento de Química Física, Universidad de Extremadura, 06071 Badajoz, Spain

ABSTRACT: Issues such as mode selectivity and Polanyi rules are connected to the effects of vibrational and translational energy in dynamics studies. Using the heavy−light−heavy OH(ν) + NH_3(ν) gas-phase reaction, these effects were analyzed by performing quasi-classical trajectory calculations, at low and high collision energies (3.0 and 10.0 kcal mol^{-1}), based on an analytical potential energy surface developed by our group. While the independent vibrational excitation of the NH_3(ν) modes increases the reactivity by a factor of ∼1.1−2.8 with respect to the vibrational ground-state at both collision energies, OH(ν) stretching acts as a spectator mode. With respect to mode selectivity, we find a different behavior for both reactants. Thus, while the OH(ν) vibrational excitation is maintained in the products, indicating a certain degree of mode selectivity, the vibrational excitation of the NH_3(ν) modes is not retained in the products; furthermore, the independent excitation of the N−H asymmetric and symmetric stretch modes leads to similar reaction probabilities, indicating negligible mode selectivity. For this early transition state reaction, translational energy is more effective in driving the reaction than an equivalent amount of energy in vibration, thus extending the validity of Polanyi rules to this polyatomic system. Finally, these results were interpreted on the basis of the existence of little or negligible intramolecular vibrational redistribution in the reactants before collision, while the nonconservation of the zero-point energy has a strong influence.

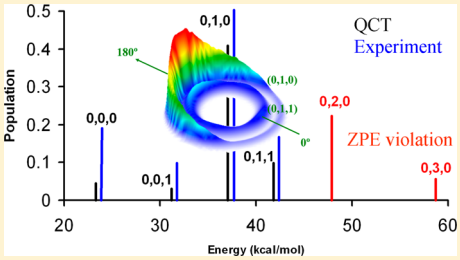

1. INTRODUCTION

The dynamics of vibrationally excited polyatomic reactions has focused the attention of a growing number of researchers in recent years due to the development of new experimental techniques and theoretical methods. In a series of pioneering studies, Zare and co-workers[1−3] and Crim and co-workers[4−6] analyzed the effects of both reactants' stretching and bending excitations on the dynamics of polyatomic systems. These dynamics studies on polyatomic reactions present a challenge both theoretically and experimentally.

Related to this issue is the problem of which motion (vibration or translation) is more effective in driving the reaction. In the simplest case, atom + diatom, this effect is straightforward to predict because only one vibrational mode is present, and the Polanyi rules[7] predict that, for a barrier located late over the course of the reaction coordinate, reactant vibrational energy can be more effective than an equivalent amount of translational energy, while the reverse is true for reactions with early transition state barriers. In the case of polyatomic systems, these concepts are more complex due to the larger number of vibrational modes involved and the possibility of energy flow between them, an effect known as intramolecular vibrational redistribution (IVR).[8]

In the case of polyatomic systems, this problem has been studied in gas−surface reactions,[9−13] atom + triatom reactions,[14] and atom + polyatom reactions,[15−17] with contradictory results. For example, Zhang and Light[14] using quantum calculations for the H + HOD reaction (which presents a late barrier on the reaction path) found that vibrational excitation is more effective in promoting the reaction than an equivalent amount of translational energy, thus apparently extending the validity of the Polanyi rules to this atom + triatom system. However, Liu and co-workers[15] in an experimental study of the reaction of Cl atoms with CHD_3 (which also presents a late barrier) found contradictory results. Recently our group also found contradictory results when analyzing the analogue F + CH_4 and F + CH_2D_2 reactions.[16,17] Using quasi-classical trajectory (QCT) calculations on a potential energy surface (PES) developed by our group,[18] we found that for these early transition state reactions, although the F + CH_4 reaction was consistent with an extension of Polanyi rules, the F + CH_2D_2 reaction showed the opposite behavior, which was interpreted on the basis of strong coupling between vibrational modes, related to IVR. On the basis of these studies, we conclude that the simple dynamics picture deduced from the diatomic molecule cases, the spectator model, and Polanyi rules does not directly carry over to the polyatomic systems, where the situation is more complex due to the greater number of degrees of freedom involved.

To shed more light on these dynamics problems, we focused our attention on the OH(ν) + NH_3(ν) → H_2O(ν) + NH_2(ν) gas-phase reaction. This exothermic reaction, with an early transition state, evolves with maxima and minima on the reaction path. We recently developed an analytical full-dimensional potential energy surface, named PES-2012,[19] which is basically a valence bond-molecular mechanics (VB-

Received: April 11, 2013
Revised: May 27, 2013
Published: May 30, 2013

MM) surface with adjustable parameters fitted exclusively to high-level ab initio calculations, at the CCSD(T)=FULL/aug-cc-pVTZ//CCSD(T)=FC/cc-pVTZ single-point level. Kinetically, we found[19] first that the forward thermal rate constants reproduce the experimental measurements in the wide temperature range 200−2000 K,[20,21] and second, that the scarce experimental reverse rate constants must be re-evaluated. Dynamically, we found[22] that, at room temperature, most of the available energy appeared as H_2O product vibrational energy (54%), reproducing the only experimental evidence.[23]

The main objectives of the present work were 2-fold: first, to analyze the effects of the reactants $OH(\nu)$ and $NH_3(\nu)$ vibrational excitations on $OH(\nu) + NH_3(\nu) \rightarrow H_2O + NH_2$ reaction dynamics; and second, to test the difficulties involved in the direct application of Polanyi rules to polyatomic reactions.

The article is structured as follows. Section II briefly outlines the potential energy surface and the energetic and computational details of the quasi-classical trajectory (QCT) method for the dynamics study. Section III presents the QCT dynamics results, and finally, the conclusions are presented in section IV.

2. THEORY AND COMPUTATIONAL DETAILS

2.1. Potential Energy Surface. Exclusively on the basis of high-level ab initio calculations, we recently developed the first analytical potential energy surface, named PES-2012, for this polyatomic system.[19] We found that the ab initio information used in the fit was reasonably reproduced by the new PES-2012 surface, especially the barrier height and the depth of the wells in the entry and exit channels. All calculations in the present article were performed on this surface, which is symmetric with respect to the permutation of the ammonia hydrogen atoms, a feature of special interest for dynamics calculations. Functional form was developed in the mentioned study and so will not be repeated here. Basically, it consists of three LEP-type (London−Eyring−Polanyi) stretch terms (str) describing the N−H bonds, augmented by valence (val) bending terms, and two functions describing the H_2O: a Morse function to describe the $O-H_j$ bond and a harmonic bending term to describe the H_i-O-H_j bending mode in water, together with a series of switching functions to permit the smooth change from pyramidal NH_3 to planar NH_2 product in the hydrogen abstraction reaction. This surface has been tested previously,[19,22] and good agreement was found with the available (though scarce) kinetics and dynamics experimental data. The surface presents an adiabatic barrier (i.e., zero-point energy included) of 2.0 kcal mol^{-1}, and a reaction enthalpy at 0 K of −11.5 kcal mol^{-1}, reproducing the ab initio values used in the fitting. In addition, it presents two deep wells, one in the entry valley, stabilized at 1.5 kcal mol^{-1} with respect to the reactants, and another in the exit channel, stabilized at 3.6 kcal mol^{-1} with respect to the products.

Formally, the total energy available to reaction is

$$E_{avail} = \Delta E_{int} + E_{coll} + \Delta E_R \quad (1)$$

where ΔE_{int}, E_{coll}, and ΔE_R are, respectively, the variation of internal energy of the reaction, the collision energy, and the reaction energy. So, only encounters with E_{avail} above the adiabatic threshold, 2.0 kcal mol^{-1}, will result in products.

The harmonic vibrational frequencies of reactants and products obtained using the PES-2012 surface are listed in Table 1. Ammonia belongs to the C_{3v} point group and has six vibrational degrees of freedom, which have only four unique frequencies. Of these six vibrational modes, there are two doubly degenerate modes with frequencies ν_1 and ν_3, and two nondegenerate modes with frequencies ν_2 and ν_4. The four modes with unique frequencies ν_1, ν_2, ν_3, and ν_4 are listed in Table 1. So, when these modes are individually excited by one quantum, extra energy is added to the reactants, from 2.9 kcal mol^{-1} for the umbrella mode (ν_4), to 10.5 kcal mol^{-1} for the asymmetric NH stretch mode (ν_1). In the $OH(\nu)$ case, the extra energy is 11.0 kcal mol^{-1}.

Table 1. Harmonic Vibrational Frequencies (in cm^{-1}) with the PES-2012[a]

NH_3	OH	NH_2	H_2O
3687 (e) (ν_1)	3805	3559 (ν_1)	3806 (ν_1)
3286 (ν_2)		3306 (ν_2)	3762 (ν_2)
1556 (e) (ν_3)		1433 (ν_3)	1651 (ν_3)
1008 (ν_4)			

[a] ν_1, ν_2, ν_3, and ν_4 correspond, respectively, to the asymmetric sretch, symmetric stretch, bending, and umbrella mode. Note that spectroscopically the vibrational state of NH_3 is labeled as ν_1, ν_4, ν_2, and ν_3. For NH_2: ν_1, ν_2, and ν_3.

2.2. Quasi-Classical Trajectory Calculations. QCT calculations[24−28] were carried out using the VENUS96 code,[29] customized to incorporate analytical potential energy surfaces. The accuracy of the trajectory was checked by the conservation of total energy and total angular momentum. The integration step was 0.03 fs, with an initial separation between the OH and the NH_3 molecules centers of mass of 10.0 Å. The trajectories were finished when the O−N distance was greater than 11.0 Å.

For each reaction considered in this work, namely, with $OH(\nu)$ and $NH_3(\nu)$ in their vibrational ground-state and with stretching and bending modes vibrationally excited, at the two collision energies considered, batches of 30 000 trajectories were calculated in which the impact parameter, b, was sampled by $b = b_{max}R^{1/2}$, with R being a random number in the interval [0, 1]. At each energy, the maximum value of the impact parameter, b_{max}, was obtained by calculating batches of 10 000 trajectories at fixed values of the impact parameter b, and systematically increasing the value of b until no reactive trajectories were obtained. The maximum value ranged between 2.6 and 3.3 Å (2.8−2.9 Å for the OH + NH_3 vibrational ground-state) at collision energy of 10.0 and 3.0 kcal mol^{-1}, respectively.

For direct comparison with our previous $OH(\nu = 0) + NH_3(\nu = 0)$ vibrational ground-state study,[22] we also calculated the NH_3 rotational energy as a Boltzmann distribution at 298 K, while for the OH reactant the rotational quantum number was fixed at a value of 0. Finally, in the present article two collision energies were analyzed: 3.0 and 10.0 kcal mol^{-1}, as an example of low and high energy regime. In total, about 5.0 × 10^5 trajectories were run.

The reaction probability, $P_r = N_r/N_T$, is the ratio of the number of reactive trajectories to the total number of trajectories, while the reaction cross-section is defined as

$$\sigma_r = \pi b_{max}^2 (N_r/N_T) \quad (2)$$

Because of the large number of trajectories run, the sampling in terms of impact parameter and rovibrational states is good enough to allow one that the results do not depend on the averaging method. Therefore, eq 2 can be applied despite its simplicity.

dx.doi.org/10.1021/jp403571y | J. Phys. Chem. A 2013, 117, 5042−5051

A serious drawback[30] of the QCT methods is that vibrational energy for a particular mode can fall below its zero-point energy (ZPE). It is well-known that there is no single correct way of incorporating this ZPE issue in trajectory calculations, several methods having been reported in the literature.[30] In order to partially correct the ZPE problem, we employ here a passive method,[31] which consists of running the trajectories with no quantum constraint and later analyzing the trajectories and discarding those that are not permitted in a quantum mechanical world. However, when applying passive methods, we must be very cautious since they perturb the statistics and therefore can lead to uncertainties in the dynamics study.[32,33]

The correct determination of the number of reactive trajectories, N_r, and the total number of trajectories, N_T, in eq 2 must be made taking into account the ZPE problem. For a direct comparison with our previous study on the vibrational ground-state,[22] here we use two ways for dealing with the ZPE issue in the trajectory calculations, out of an infinite number of possibilities: (a) All trajectories are included in the analysis of the results. This is the conventional way of performing QCT calculations. This method is known as standard binning (or histogram procedure) with all trajectories, SB-All. (b) Trajectories, for which the products' or reformed reactants' vibrational energy is less than the ZPE, are not included in the analysis of the results. This method is called standard binning (or histogram procedure) with double ZPE constraint, SB-DZPE. Note that this approach is similar to Nyman and Davidsson's[34] ZP3 method and to Varandas'[35] IEQMT approach.

2.3. Determination of Intramolecular Vibrational Redistributions and Vibrational State Distributions. To obtain information on the intramolecular vibrational redistribution (IVR) in the reactant channel before the collision between reactants and on the $H_2O(\nu)$ and $NH_2(\nu)$ products vibrational distributions, two original modifications[36] were made to VENUS96. Since VENUS uses a space fixed frame, a change to a body fixed frame is necessary for these analyses. So these calculations are preceded by a rotation and translation of the molecules (reactants in the first case and products in the second) in order to maintain the orientation of the respective reference equilibrium geometry (X^{eq}).

We begin by analyzing the common part in both cases. Assuming the validity of a harmonic independent normal mode treatment, the vibrational energy deposited on the ith normal mode, E^i_{har}, is computed as the sum of a kinetic, $E^i_{kin,har}$, and a potential energy, $E^i_{pot,har}$.

$$E^i_{har} = E^i_{kin,har} + E^i_{pot,har} \tag{3}$$

Kinetic energy is computed using the vector of linear momenta in unscaled Cartesian coordinates projected onto the normal mode space. Thus, if $P_{l\gamma}$ is the γ component ($\gamma = x, y, z$) of the momentum of the l atom, and $c^i_{l\gamma}$ is the $l\gamma$ component of the Ith normal mode eigenvector, one has

$$E^i_{kin,har} = \frac{1}{2}[P_i(s)]^2 = \frac{1}{2}\left(\sum_{l=1}^{N}\sum_{\gamma=1}^{3} c^i_{l\gamma}p_{l\gamma}\right)^2 \tag{4}$$

Note that the mass factor in the kinetic energy cancels out since we are using unscaled Cartesian momenta and mass-weighted normal mode eigenvectors. So, the total kinetic energy is exact and is the same as the kinetic energy in Cartesian coordinates.

In the harmonic approximation, potential energy is computed as

$$E^i_{pot,har} = \frac{1}{2}(\omega^i\Delta^i)^2 \tag{5}$$

with ω^i being the frequency of the ith mode and Δ^i the displacement along the ith normal mode. This displacement is obtained from the differences between the equilibrium unscaled Cartesian coordinates vector, X^{eq}, and the unscaled Cartesian coordinates of the fragment at the final step of the trajectory, X, projected onto the normal mode space, so that

$$\Delta^i = \sum_l \sum_\gamma (X_{l\gamma} - X^{eq}_{l\gamma})c^i_{l\gamma}M_l \tag{6}$$

with M_l being the mass of the lth atom. This mass accounts for the transformation from mass-weighted to unscaled Cartesian coordinates and introduces the correct reduced mass of vibration in eq 5.

This calculation is performed for each trajectory, and in these modifications, the rotational motion of the polyatomic system is not considered, and so the vibrational and rotational motions are treated independently. Finally, note that in the IVR calculation the X^{eq} term in eq 6 refers to the OH and NH_3 reactants, while in the vibrational distribution it refers to the H_2O and NH_2 products.

First, for the study of IVR in the $NH_3(\nu)$ reactant, batches of 1000 trajectories were run, and in this case, the reference equilibrium geometry (X^{eq} in eq 6) corresponds to the NH_3 reactant. The initial conditions were set in such a way as to ensure that no interaction between the reactants took place in the course of the period of time examined in these trajectories. Thus, the separation between the reactant centers of mass is now larger, 15.0 Å, and the impact parameter is fixed at 10.0 Å (compare with the b_{max} = 2.8−2.9 Å for the OH + NH_3 vibrational ground-state calculated previously). In this case, the trajectories are asymptotic trajectories, i.e., without interaction with the reactant partner.

Each set of trajectories was independently run for the $OH(\nu)$ + $NH_3(\nu)$ vibrational ground-state and for different stretching and bending excitations by one quantum, and the energy for each normal mode was averaged for all trajectories in each case. The variation in each normal mode's average energy was taken as an indication of the internal flow of energy between normal modes in $NH_3(\nu)$. Note that this energy flow occurs before the collision between both reactants, so that it is not related to the mode−mode coupling along the reaction path (Coriolis-like terms),[37] which is a qualitative indication of the energy flow when a reactive collision occurs.

Second, to assign a discrete quantum-like vibrational state to the outcome of a QCT calculation, we adopted the NMA (normal-mode analysis) algorithm recently developed by our group for polyatomic systems.[36] This method has a lower computational cost than the fast Fourier transform method,[38,39] while yielding similar results. In this case, the reference equilibrium geometry (X^{eq} in eq 6) corresponds to the $H_2O(\nu)$ and $NH_2(\nu)$ products. Therefore, the energy in each normal mode was computed from eq 3, and assuming harmonic approximation, the action variable, n_i, is calculated from the vibrational energy and harmonic vibrational frequency using the well-known expression

$$E^i_{har} = E^i_{vib} = \left(n_i + \frac{1}{2}\right)\hbar\varpi_i \tag{7}$$

rounded to the closest integer to obtain the vibrational quantum number of mode i.[36]

dx.doi.org/10.1021/jp403571y | J. Phys. Chem. A 2013, 117, 5042−5051

Since harmonic approximation was used for this calculation, a breakdown of the procedure for highly excited states could have been expected. However, since we are interested in the lowest product vibrational states, it can be assumed that this method is sufficiently accurate for the present purpose.

2.4. Hamiltonian Reaction-Path and Coupling Terms. The mode−mode coupling along the reaction path (Coriolis-like terms) was analyzed using the reaction-path Hamiltonian.[37] Kinetic energy is given by

$$T(s, p_s, \{Q_i(s)\}, \{Pi(s)\}) = \frac{1}{2\mu}\sum_{i}^{3N-7} P_i^2(s) + \frac{1}{2\mu}\frac{\left[p_s - \sum_{i=1}^{3N-7}\sum_{i'=1}^{3N-7} Q_i(s)P_{i'}(s)B_{ii'}(s)\right]^2}{\left[1 + \sum_{i=1}^{3N-7} Q_i(s)B_{iF}(s)\right]^2} \quad (8)$$

where p_s and $P_i(s)$ are the momenta conjugate to the reaction coordinate s and the $3N - 7$ orthogonal normal-mode coordinates $Q_i(s)$, respectively. In this expression, $B_{iF}(s)$ and $B_{ii'}(s)$ are the so-called coupling terms over the course of the reaction coordinate. The first, $B_{iF}(s)$, is the term measuring the coupling between the normal mode i and the motion over the course of the reaction coordinate, F,

$$B_{iF}(s) = -\sum_{l\gamma=1}^{N} \frac{d\nu_{l\gamma}(s)}{ds} c_{l\gamma}^{i}(s) \quad (9)$$

where $\nu_{l\gamma}(s)$ is the $l\gamma$ component of the normalized gradient vector, and $c_{l\gamma}^{i}(s)$ is the $l\gamma$ component of the eigenvector for mode i. These terms are the components of the reaction path curvature, $\kappa(s)$, defined as

$$\kappa(s) = \left(\sum [B_{iF}(s)]^2\right)^{1/2} \quad (10)$$

and they control the nonadiabatic flow of energy between these modes and the reaction coordinate.[40] Interest in the calculation of these coupling terms lies in the qualitative explanation of the possible vibrational excitation of reactants and products. So, the larger the term is, the larger the flow of energy between the mode i and the reaction coordinate, indicating the excitation of this mode would greatly enhance the reaction rate.

The $B_{ii'}(s)$ terms are the Coriolis-like coupling terms between modes, given by

$$B_{ii'}(s) = \sum_{l\gamma=1}^{N} \frac{dc_{l\gamma}^{i}(s)}{ds} c_{l\gamma}^{i'}(s) \quad (11)$$

and they provide information about the energy flow between the vibrational modes in the reaction process. So, a large $B_{ii'}(s)$ term indicates that the energy initially deposited in mode i can flow to mode i'.

Note that a shortcoming of the reaction path Hamiltonian analysis is that it does not include coupling between vibration and rotation, which can lead to coupling between symmetric and asymmetric vibrational modes of a molecule.[41] The Hamiltonian reaction path and the $B_{iF}(s)$ terms were calculated with the POLYRATE code,[42] and the $B_{ii'}(s)$ terms were calculated with a purpose-designed code, which uses information from the output file of POLYRATE.

3. RESULTS AND DISCUSSION

3.1. Effect of the Vibrational Excitation on the Reactivity. The QCT reaction cross-sections with respect to the OH(ν) + NH_3(ν) vibrational ground-state for all vibrational excitations considered independently in this work, namely, ν_1, ν_2, ν_3, and ν_4 of NH_3(ν) and OH(ν = 1), are listed in Table 2 at two collision energies, 3.0 and 10.0 kcal mol^{-1}.

Table 2. QCT Reaction Cross-Sections with Respect to OH + NH_3 Vibrational Ground-State (gs) on the PES-2012 Surface at Two Collision Energies, for Different NH_3(ν) and OH(ν) Vibrational Excitations; Values Correspond to the SB-All Approach, and Values in Parentheses Correspond to the SB-DZPE Approach; Maximum Error Bar ±0.1

	σ_v/σ_{gs}	
NH_3 vibrational mode excited	3.0 kcal mol^{-1}	10.0 kcal mol^{-1}
ν_1 (asymm. stretch)	2.8(2.0)	1.4(1.4)
ν_2 (symm. stretch)	2.8(1.7)	1.4(1.1)
ν_3 (bending)	1.7(1.4)	1.1(0.8)
ν_4 (umbrella)	1.4(0.4)	1.1(0.7)
OH vibrational mode excited	1.0(0.2)	1.0(0.4)

We began by analyzing the behavior of the OH vibrational excitation, which supposedly acts as a spectator mode (see below). While the SB-All approach supports this supposition, where the reaction cross-section is indifferent to the vibrational excitation, σ_v/σ_{gs} = 1.0, at the two collision energies; the SB-DZPE approach indicates that the excitation of this mode strongly inhibits the reactivity with respect to the vibrational ground-state, σ_v/σ_{gs} = 0.2−0.4.

Given these differences using different approaches to solve the ZPE problem, we performed a detailed analysis of the trajectories to explore this issue more deeply. Thus, while in the SB-All approach, all trajectories (reactive and nonreactive) in the reaction probability, $P_r = N_r/N_T$, were considered, in the SB-DZPE approach the DZPE criterion was applied in the numerator and denominator of the reaction probability, and this has a strong influence on the denominator, N_T. Remember that N_T is the total number of trajectories minus the number of reactive trajectories whose final vibrational energy is below the ZPE of the two products, H_2O and NH_2, and minus the number of nonreactive trajectories whose final vibrational energy is below the ZPE of the two reactants, OH and NH_3. Thus, for the title reaction, while in the OH(ν = 1) case, 69% of nonreactive trajectories appeared with the vibrational energy of the two reactants below their ZPE (i.e., did not fulfill the DZPE criterion), in the ground-state, this percentage increased to 94%. As this amount subtracts from the denominator, it makes the fraction artificially larger for the ground-state case. Thus, for this vibrational/ground-state comparison, the SB-DZPE criterion is too restrictive and will not be used in the remainder of the article.

With regard to the other reactant, by using the SB-All approach at low and high energies (3.0 and 10.0 kcal mol^{-1}), we found that the NH_3(ν) vibrational excitation of all modes increased the reactivity with respect to the ground-state by factors 2.8−1.1 and was more important for the NH stretching modes (ν_1 and ν_2) and for low collision energy. To gain further insight into this behavior, we analyzed the reaction path curvature, κ(s) (eq 10), which measures the coupling between the normal modes and the reaction coordinate (Figure 1). We found a coupling between the reaction coordinate and the N−

dx.doi.org/10.1021/jp403571y | J. Phys. Chem. A 2013, 117, 5042−5051

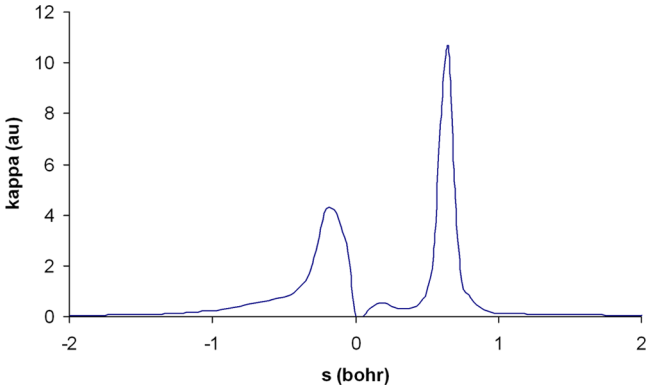

Figure 1. Reaction path curvature, κ, as a function of reaction coordinate, s.

H symmetric stretch mode (broken bond) in the entry channel (s = −0.15 bohr), and a stronger coupling of the reaction coordinate to the O−H stretching mode of water (new formed bond) in the exit channel (s = +0.65 bohr). Therefore, with this simple mode-selective picture, we would expect a priori that excitation of the OH(ν) mode does not influence reactivity, whereas excitation of this $NH_3(\nu)$ stretch mode would enhance reactivity with respect to the vibrational ground-state; this is in fact the behavior observed at 3.0 and 10.0 kcal mol^{-1}. Analysis of the reaction path curvature also supports the previous supposition that the reactant OH(ν) stretching mode acts as a spectator mode.

Unfortunately, no experimental information is available for comparison, and only one theoretical study[43] has been previously reported. Nyman reported reduced-dimensionality quantum scattering calculations based on a simplified PES, where the NH_2 fragment is treated as a pseudoatom, and found that the vibrational excitation of the N−H stretch mode increases the reactivity by factors 2.0 and 1.9 at 3.0 and 10.0 kcal mol^{-1}, respectively. In spite of the great differences between both studies (method and PES), both results reproduce the same behavior, where an increase in reactivity is observed with the N−H vibrational excitation, and is most important at low energies.

3.2. N−H Symmetric and Asymmetric Comparison: an Example of Coupling Modes. On the PES-2012 surface, analysis of the reaction path curvature[37] (eq 10, Figure 1) shows that, while the N−H symmetric stretch mode (ν_2) is strongly coupled to the reaction coordinate, the N−H asymmetric stretch mode (ν_1) is not. Given that the reaction path curvature indicates that excitation of a given mode would greatly enhance the reactivity, with this simple mode-selective picture, one could a priori expect a great difference in reactivity between the two stretch mode excitations, and possibly even a change in their dynamics. However, the QCT results show that both modes (ν_1 and ν_2) present similar reactivity at low and high collision energies (Table 2).

To understand the effects of the asymmetric and symmetric excited N−H stretch modes of $NH_3(\nu)$, which differ by 401 cm^{-1}, we shall analyze the IVR before the collision between OH and NH_3 took place. Figure 2 plots the temporal evolution of the energy available in different modes of the ground-state NH_3 reactant (panel a), and after the NH asymmetric (ν_1, panel b) and NH symmetric (ν_2, panel c) stretch modes were independently excited by one quantum, averaged over all asymptotic trajectories. We shall begin by discussing the

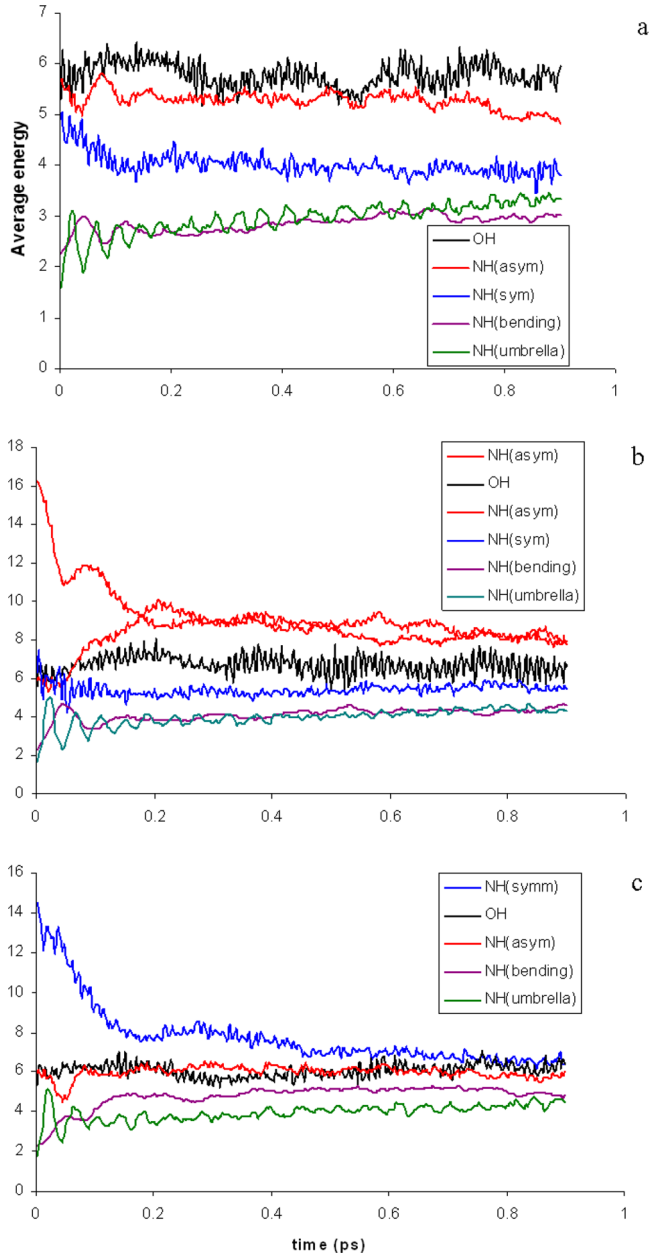

Figure 2. Average energy (kcal mol^{-1}) of each normal mode from QCT calculations as a function of time. Panel a shows the results for the vibrational ground state; panel b for excitation of the N−H asymmetric stretching mode by one quantum, ν_1 = 1; and panel c for excitation of the N−H symmetric stretching mode by one quantum, ν_2 = 1.

vibrational ground-state (panel a). According to our classical trajectory calculations, the different modes practically maintain their adiabaticity until interaction with the OH, with a small energy flow from the NH symmetric (ν_2) mode to the bending (ν_3) and umbrella (ν_4) modes. Note that there is a broad region in energy where vibrational energy remains localized to modes of the molecule prior to reaction, as observed here, even for polyatomics much larger than NH_3.[44,45]

When the NH asymmetric (panel b) and NH symmetric (panel c) are independently excited by one quantum, they are fast deactivated ($t \approx 0.2$ ps), the energy is transferred to the lowest modes, and therefore, the energy of the two modes tends to be similar. Therefore, a part of the energy originally

dx.doi.org/10.1021/jp403571y | J. Phys. Chem. A 2013, 117, 5042−5051

deposited into one mode flows to other modes and thus loses its reaction effectiveness. Therefore, the reaction does not preserve vibrational adiabaticity along the reaction, indicating that this reaction does not exhibit clear mode selectivity. Moreover, these results show that in the case of polyatomic systems, with various degrees of vibrational freedom, the situation is more complex than that obtained exclusively from a naive picture of coupling terms.

In this analysis, three points of caution need to be taken into account. First, this time scale can not be directly compared with the time scale for the reactive trajectories because in the IVR case the initial separation between reactants is larger, and the initial conditions are set to ensure that no reaction takes place. Second, a known error in classical trajectories is that IVR is much faster than it should be, and so energy channelled to a given vibrational mode easily flows to different modes. Third, it should be borne in mind that this correlation between the classical trajectory results and quantum states is somewhat artificial since, contrary to our classical calculations, in a quantum mechanical world the transfer of infinitesimal amounts of energy is forbidden. However, quantum mechanically the wave function can be a superposition of several eigenstates and, thus with a certain degree of probability, represent an excited state even though the energy is less than that of the excited state. Nonetheless, these caveats can help to understand the QCT results.

Unfortunately, no experimental/theoretical information is available for comparison in the title reaction, but this behavior agrees with the results for the Cl + CH_4 reaction, both experimentally[1] and theoretically,[46] where the reactivity resulting from the two vibrationally excited modes (symmetric and asymmetric C−H stretch mode) are found to be practically indistinguishable.

3.3. Mode Selectivity. Taking as an illustrative textbook example the H + H_2O → H_2 + OH reaction, the vibrational excitation initially prepared in the nonreactive OH bond of the reactant could survive the reaction and appear in the OH product. Thus, the vibrational excitation of one OH bond produces only OH(ν = 0), while the vibrational excitation of the two OH bonds produces OH(ν = 1).

We begin the study of this property by considering the product energy partitioning. The QCT product energy partitioning at two collision energies on the PES-2012 surface is listed in Table 3, where f_v, f_r, and f_t are the fractions of the available energy appearing in vibration, rotation, and translation, respectively. First, we began by analyzing the behavior of the OH(ν = 1) vibrational excitation. At low and high collision energy (3.0 and 10.0 kcal mol^{-1}), the vibrational excitation of this mode increased the H_2O vibrational fraction with respect to the vibrational ground-state (∼20%), i.e., it survives the reaction, indicating a certain degree of selectivity. Second, in the $NH_3(\nu)$ case, the vibrational excitation by one quantum in the lowest modes, ν_3 and ν_4, did not survive the reaction at low and high collision energies. However, when the ν_1 and ν_2 modes were independently excited by one quantum at low and high collision energies, a certain degree of selectivity was found.

To explore this issue in a more quantitative way, we analyzed in Figures 3 and 4 the vibrational populations in the products when different OH(ν) and $NH_3(\nu)$ reactant modes were individually excited by one quantum. Given the similar behavior found with the collision energy, in this section, we consider the lowest energy, 3.0 kcal mol^{-1}. First, we studied the vibrational population in the $NH_2(l,m,n)$ product (Figure 3), where l and m are the quantum numbers for the N−H asymmetric and symmetric stretch modes (ν_1 and ν_2), and n is that for the bending mode (ν_3). Starting from the OH(ν = 0) + $NH_3(\nu$ = 0) reactants ground-state, the $NH_2(\nu)$ appeared practically in its vibrational ground-state (0,0,0), ∼70%, with ∼18% in the bending mode (0,0,1) (panel a). This result agrees with the low product vibrational fraction obtained (Table 3). When the N−

Table 3. QCT Product Energy Partitioning (in Percentages), at Two Collision Energies, When Different $NH_3(\nu)$ and OH(ν) Vibrational Modes Are Independently Excited by One Quantum

	$f_v(NH_2)$	$f_r(NH_2)$	f_t	$f_v(H_2O)$	$f_r(H_2O)$
E_{coll} = 3.0 kcal mol^{-1}					
ground state	17	6	15	56	5
$NH_3(\nu_1 = 1)$	23	5	13	53	6
ν_2 = 1	21	5	13	55	6
ν_3 = 1	19	5	13	57	6
ν_4 = 1	15	6	16	57	6
OH(ν = 1)	11	3	9	74	3
E_{coll} = 10.0 kcal mol^{-1}					
ground state	13	6	35	39	6
$NH_3(\nu_1 = 1)$	22	5	26	39	7
ν_2 = 1	20	5	27	40	7
ν_3 = 1	16	6	31	40	7
ν_4 = 1	14	7	34	39	7
OH(ν = 1)	9	4	25	57	5

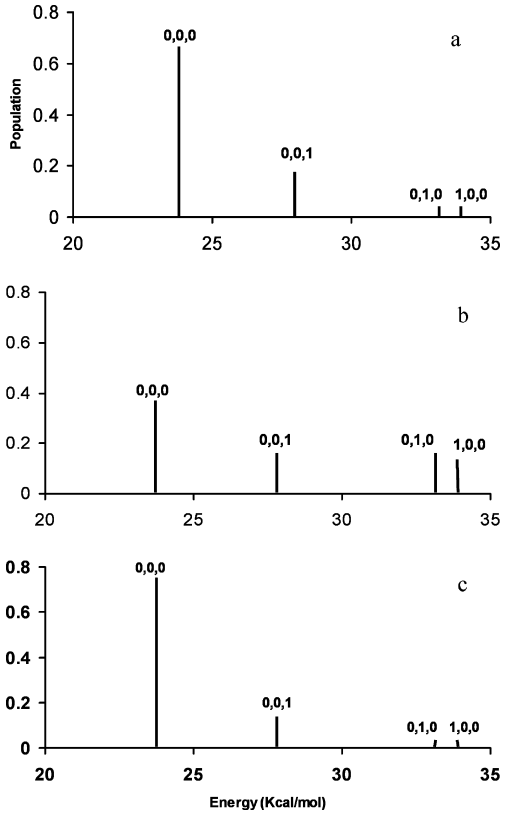

Figure 3. Vibrational state distribution of the $NH_2(l,m,n)$ product at collision energy of 3.0 kcal mol^{-1}. Panel a: starting from the OH(ν = 0) + $NH_3(\nu$ = 0) ground-state. Panel b: starting from the OH(ν = 0) + $NH_3(\nu_2$ = 1) state. Panel c: starting from the OH(ν = 1) + $NH_3(\nu$ = 0) state. Note that only the most populated states are shown and that the y-axis scale is the same for a direct comparison.

dx.doi.org/10.1021/jp403571y | J. Phys. Chem. A 2013, 117, 5042−5051

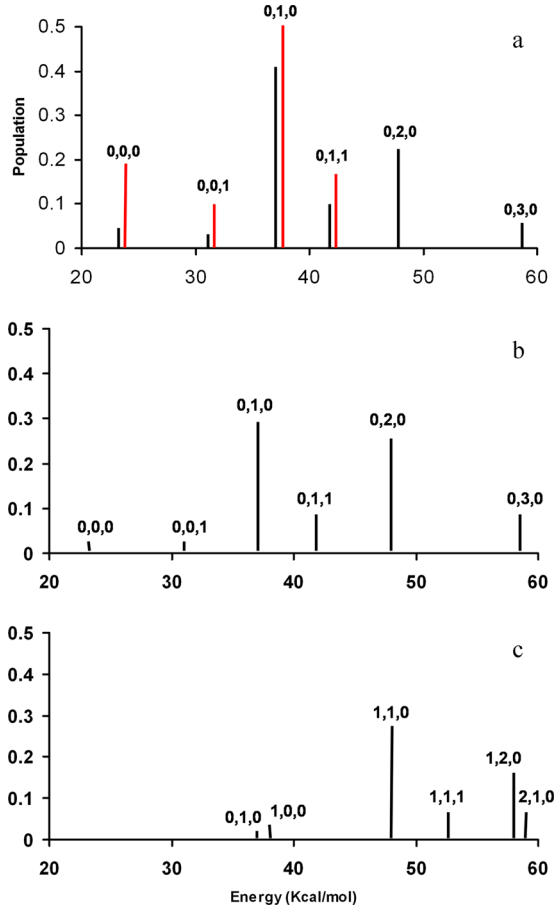

Figure 4. Same as that n Figure 3, but for the vibrational state distribution of the $H_2O(l,m,n)$ product. In red are the values from the experiment.[23]

H symmetric stretch mode is excited in the NH_3 reactant (panel b), the NH_2 product appears largely excited, where the ground-state population (0,0,0) decreases from ∼70% to ∼40%. The main changes appeared in the N−H stretching modes (ν_1 and ν_2), which increased from 1−4% to 12−14%. Thus, the energy originally deposited in the N−H symmetric stretch mode of the NH_3 reactant is distributed between different modes in the NH_2 product, due to $B_{ii'}(s)$ (eq 11) couplings in the exit channel. Consequently, the vibrational excitation initially prepared in the reactive N−H symmetric mode practically does not survive the reaction, indicating that this reaction only partially exhibits mode selectivity. However, the excitation of the reactant OH(ν = 1) by one quantum does not modify practically the original distribution (panel c), revealing once again the behavior of this mode as a spectator mode.

Second, we analyzed the vibrational population in the $H_2O(l,m,n)$ coproduct (Figure 4) and compared it with the only experimental data available.[23] Note that this comparison is only approximate because, while the experimental data were recorded from a fast-flow reactor at 298 K, the QCT results were obtained at low collision energy, 3.0 kcal mol^{-1}. However, this comparison is justified because the Boltzmann distribution of the collision energy at this temperature shows a broad peak at low energies, with the maximum at ∼1 kcal mol^{-1}.

Starting from the OH(ν = 0) + NH_3(ν = 0) reactants ground-state (panel a), the H_2O product appears vibrationally excited, mainly in the OH stretching mode, (0,m,0) m = 1−3, ∼70%, and only 4% in its ground-state (0,0,0). As compared to the experiment, the QCT results yield a hotter vibrational distribution, and we note two drawbacks associated with the QCT results. First, the low contribution of the (0,0,0) and (0,0,1) states, 7%, compared with the experiment, 29%, and second, the high contribution (27%) of the m = 2,3 states compared with the experiment (0%), are not energetically accessible. Thus, with the available energy, 15.5 kcal mol^{-1}, only states with up to one quantum in the OH stretching mode (11.0 kcal mol^{-1}) or states with one quantum in the OH stretching mode and one quantum in the H_2O bending mode (4.7 kcal mol^{-1}) can be populated from the reaction. This difference is again due to the violation of the ZPE problem. Thus, in the (0,2,0) and (0,3,0) states of H_2O, the NH_2 coproduct appears always with a vibrational energy below its ZPE (100% of reactive trajectories). There is therefore an artificial flow of vibrational energy from the NH_2 to H_2O, yielding an artificial population in the high vibrational states.

When the NH symmetric stretch mode of the NH_3 reactant is excited by one quantum (panel b), an extra energy of 9.4 kcal mol^{-1} is added, and now the available energy is 24.9 kcal mol^{-1}. With this energy, states with up to two quanta in the OH stretching mode can be populated from the reaction. Now the (0,2,0) state is real, while the (0,3,0) state is an overestimation of the QCT method due again to the violation of the ZPE problem. Thus, this mode, which is the broken-formed bond in this hydrogen abstraction reaction, only partially survives the reaction. As it was previously analyzed (Figure 2c), this can be explained because, when the NH symmetric stretch mode is excited by one quantum, it is fast deactivated ($t \approx 0.2$ ps), and the energy is transferred to the lowest modes, thus losing part of its effectiveness.

Finally, the excitation of the reactant OH(ν = 1) by one quantum shows two effects (panel c). First, it increases the number of excited states in the H_2O product, where the ground-state population (0,0,0) decreases from 5% to ∼0%, and second, the energy originally deposited in the reactant O−H stretch mode partially survives in the product, indicating its character of spectator mode.

To shed more light on the dynamics of this reaction, we finish this section analyzing the triple angle-velocity differential cross-sections in different vibrational states (0,1,0) + (0,1,1) of the H_2O product from the OH(ν = 0) + NH_3(ν = 0) reactants vibrational ground-state, which, as previously seen, is the only state experimentally analyzed (Figure 5). This surface plot is obtained from the product translational energy distributions and center-of-mass angular distributions of QCT calculations.

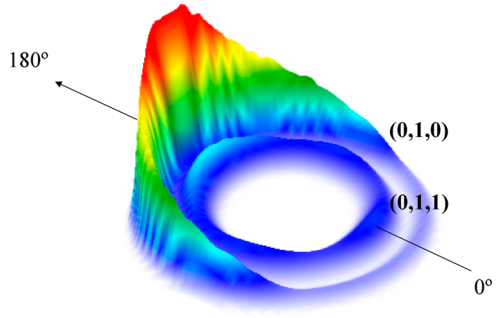

Figure 5. QCT polar scattering 3D surface plot of the CM scattering angle-velocity distribution, $P(\omega,\theta)$, for the $H_2O(l,m,n)$ product of the OH(ν = 0) + NH_3(ν = 0) reaction at 3.0 kcal mol^{-1}.

dx.doi.org/10.1021/jp403571y | J. Phys. Chem. A 2013, 117, 5042−5051

While the (0,1,0) state (outer circle) presents a clear backward scattering distribution, associated with a rebound mechanism and low impact parameters, the (0,1,1) state (inner circle) shows an isotropic behavior, with a very light forward−backward tendency. Unfortunately, there are no experimental data for comparison. Therefore, these results can be used as a test in future experimental or theoretical studies on the title reaction.

3.4. ZPE Problem: Influence of the Counting Method. To analyze the theory/experiment differences found in the $H_2O(l,m,n)$ product vibrational distributions starting from the $OH(\nu = 0) + NH_3(\nu = 0)$ vibrational ground-state reaction, we tested several alternatives to deal with vibational quantization in the products. (a) Once we obtained the real vibrational actions, they were rounded to the nearest integer, i.e., actions between 0.5 and 1.5 were assigned to a vibrational quantum number of 1. This is the approach used in this article and described in section 2.3. (b) We took as vibrational quantum number the truncated integer of the real vibrational actions, i.e., actions between 0.0 and 1.0 were assigned to 0. Note that these two approaches use the standard binning (SB) counting method. (c) We also tested the Gaussian weighted binning (GB) procedure[33] where the actions close to integer values are considered by Gaussian-weighting the trajectories so that the closer the final actions are to integer values, the larger the weights. (d) These three alternatives consider the whole number of reactive trajectories. Finally, to avoid the artificial flow of energy from NH_2 to H_2O, a drastic alternative to consider is the SB-DZPE approach (section 2.2), where the NH_2 and H_2O products appear always above their ZPEs. Note, however, that we have shown (section 3.1) that this alternative is too restrictive for this reaction.

Figure 6 plots the $H_2O(l,m,n)$ vibrational populations using these four alternatives, together with the experimental values[23]

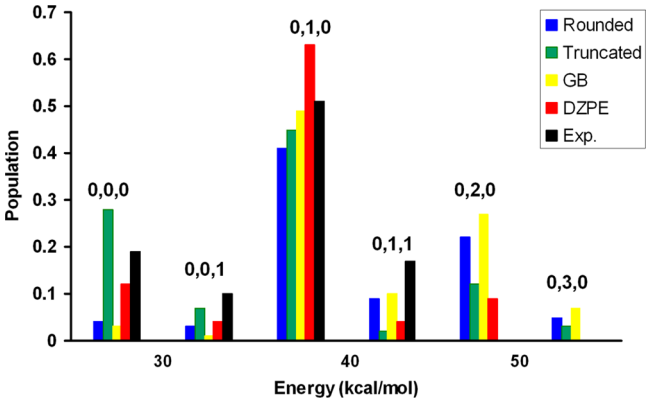

Figure 6. Vibrational state populations obtained by means of SB-rounded (blue), SB-truncated (green), GB (yellow), and SB-DZPE (red), as compared to the experimental data[23] (black). Numbers above the populations specify the states.

for comparison. Although the truncated method improves the agreement with experiment, it represents a very restrictive alternative. Moreover, this method and the GB method do not correct the overestimation of the (0,2,0) and (0,3,0) states, 15% and 34%, respectively. Obviously, the SB-DZPE method corrects this overestimation, although it does not remove it completely (9%) and in consequence overestimates the (0,1,0) population. Thus, the SB-rounded method used in this article represents a compromise between several alternatives. In sum, the binning procedure drastically affects the QCT results and only a state-to-state quantum mechanical study would be able to solve this difference with experiment.

3.5. Vibrational versus Translational Energy. As was noted in the introduction, while the application of Polanyi rules is well established in atom−diatom reactions because only one vibrational mode is present, in the case of polyatomic systems the situation is more complex, and their application is not so straightforward.

For the title reaction, with a barrier located early in the reaction path, we studied the effects of equivalent amounts of energy as vibration or translation in overcoming the reaction barrier, with different combinations of translational and vibrational energy being used for comparison. Note that, in this comparison, we are considering independently the OH mode (3805 cm^{-1}), the NH asymmetric and symmetric stretch modes (ν_1= 3687 cm^{-1} and ν_2 = 3286 cm^{-1}), and the NH_3 bending modes (ν_3 = 1556 cm^{-1} and ν_4 = 1008 cm^{-1}) at two collision energies, 3.0 and 10.0 kcal mol^{-1}. Thus, for 3.0 kcal mol^{-1}, the possible combinations are given in Table 4.

Table 4. Collision Energies and Total Engeries

	E_{coll} (kcal mol^{-1})	E_{total} (kcal mol^{-1})
$OH(\nu = 0) + NH_3(\nu_1 = 1)$	3.0	13.5
$OH(\nu = 0) + NH_3(\nu = 0)$	13.5	13.5
$OH(\nu = 0) + NH_3(\nu_2 = 1)$	3.0	12.4
$OH(\nu = 0) + NH_3(\nu = 0)$	12.4	12.4
$OH(\nu = 0) + NH_3(\nu_3 = 1)$	3.0	7.4
$OH(\nu = 0) + NH_3(\nu = 0)$	7.4	7.4
$OH(\nu = 0) + NH_3(\nu_4 = 1)$	3.0	5.9
$OH(\nu = 0) + NH_3(\nu = 0)$	5.9	5.9
$OH(\nu = 1) + NH_3(\nu = 0)$	3.0	14.0
$OH(\nu = 0) + NH_3(\nu = 0)$	14.0	14.0

Note first, that, for the collision energy of 10.0 kcal mol^{-1}, the combinations are the same, but now we must add 7.0 kcal mol^{-1} to all the values of total energy, and second, that, for clearness, the OH and NH_3 rotational energies are not included in these combinations, although they are obviously considered in the calculations.

The QCT ratios of reaction cross-sections on the PES-2012 surface are listed in Table 5 at the two collision energies. First, over the wide range of energies analyzed, 5.9 to 21.0 kcal mol^{-1}, the translational energy is most effective in driving the reaction than an equivalent amount of energy in vibration. These results are consistent with an extension of Polanyi rules to this polyatomic system with an early transition state. Second, this behavior is dependent on the collision energy, the mode excited, and the ZPE approach. Thus, for the $NH_3(\nu)$ reactant, this effect is more pronounced at low collision energies, while at high energy (10.0 kcal mol^{-1}) the translational and vibrational energies present similar effectiveness, within the error bar. With respect to the mode excited, the effect of the $OH(\nu = 1)$ becomes more important than the effect of the $NH_3(\nu)$ at both collision energies. This behavior is consistent with the supposition of the $OH(\nu = 1)$ mode as a spectator mode. Finally, the effect of the ZPE violation in QCT calculations is also important, with the SB-DZPE approach overestimating this effect practically in all vibrational modes, especially in the $OH(\nu)$ case.

dx.doi.org/10.1021/jp403571y | J. Phys. Chem. A 2013, 117, 5042−5051

Table 5. Ratio of Reaction Cross-Sections,[a] on the PES-2012 Surface, for Different Translational and Vibrational Energy[b] Combinations

vibration	translation	total	σ_t/σ_v[c]
E_{coll} = 3.0 kcal mol^{-1}			
$NH_3(\nu_1 = 1)$	3.0	13.5	1.4(1.1)
$\nu = 0$	13.5	13.5	
$\nu_2 = 1$	3.0	12.4	1.2(1.3)
$\nu = 0$	12.4	12.4	
$\nu_3 = 1$	3.0	7.4	1.5(1.1)
$\nu = 0$	7.4	7.4	
$\nu_4 = 1$	3.0	5.9	1.4(2.8)
$\nu = 0$	5.9	5.9	
$OH(\nu = 1)$	3.0	14.0	3.8(9.2)
$\nu = 0$	14.0	14.0	
E_{coll} = 10.0 kcal mol^{-1}			
$NH_3(\nu_1 = 1)$	10.0	20.5	0.9(0.9)
$\nu = 0$	20.5	20.5	
$\nu_2 = 1$	10.0	19.4	0.9(1.0)
$\nu = 0$	19.4	19.4	
$\nu_3 = 1$	10.0	14.4	1.0(1.3)
$\nu = 0$	14.4	14.4	
$\nu_4 = 1$	10.0	12.9	1.0(1.5)
$\nu = 0$	12.9	12.9	
$OH(\nu = 1)$	10.0	21.0	1.3(2.7)
$\nu = 0$	21.0	21.0	

[a]All vibrational states of the products have been considered. Values correspond to the SB-All approach, and values in parentheses correspond to the SB-DZPE approach. [b]Energies in kcal mol^{-1}. [c]Maximum error bar ±0.1.

4. CONCLUSIONS

In the present article, we have performed QCT calculations on an analytical surface, PES-2012, recently developed by our group to describe the hydrogen abstraction $OH(\nu)$ + $NH_3(\nu)$ gas-phase reaction, with the aim of analyzing the effects of $OH(\nu)$ and $NH_3(\nu)$ vibrational excitations and translational energy on the dynamics of this reaction. These effects are connected with issues such as mode selectivity and Polanyi rules.

(1) The independent one-quantum vibrational excitation of all $NH_3(\nu)$ modes increased reactivity with respect to the vibrational ground-state by factors ∼1.1−2.8, while the OH(v) reactant acted as a spectator mode. These behaviors are independent of the collision energy (3.0 and 10.0 kcal mol^{-1}). (2) The $OH(\nu)$ vibrational excitation by one-quantum was maintained in the H_2O product, suggesting that the prepared vibrational mode in the reactant survives in the product, indicating a certain degree of mode selectivity. (3) However, the independent vibrational excitation by one quantum of all $NH_3(\nu)$ modes did not remain localized in a well-defined motion on the course of the reaction and were not retained in the products. Moreover, the independent one-quantum vibrational excitations of the N−H asymmetric and symmetric stretch modes showed similar reaction probabilities. These results indicate negligible mode selectivity, this behavior being associated with fast IVR during the reaction. (4) On comparing the effects of equivalent amounts of vibrational and translational energy in driving the reaction, the QCT results showed that, for the wide energy range 5.9−21.0 kcal mol^{-1}, the translational energy was more effective than an equivalent amount of vibrational energy. This was the expected behavior for an early transition state and extends the validity of the Polanyi rules to this polyatomic system. In this case, the translational motion, parallel to the entrance valley, favors the reaction, while the vibrational excitation, with its motion orthogonal to the reaction coordinate, produces a bottleneck in the reactant region. (5) The QCT results are strongly dependent on the standard binning counting approach used to incorporate the ZPE-violation issue.

As noted by Simons,[47] bond selectivity and mode selectivity are rare events in chemistry. They depend on the target molecule and the localization in it of the vibrational modes, i.e., they are the exception and not the rule.

AUTHOR INFORMATION

Corresponding Author

*(J.E.-G.) E-mail: joaquin@unex.es.

Notes

The authors declare no competing financial interest.

ACKNOWLEDGMENTS

This work was partially supported by Gobierno de Extremadura, Spain, and Fondo Social Europeo (Project No. IB10001). M.M.-P. thanks Gobierno de Extremadura (Spain) for a scholarship. Many calculations were carried out on the LUSITANIA computer at Computaex (Spain).

REFERENCES

(1) Bechtel, H. A.; Camden, J. P.; Brown, D. J. A.; Zare, R. N. Comparing the Dynamical Effects of Symmetric and Antisymmetric Stretch Excitation of Methane in the Cl + CH_4 Reaction. *J. Chem. Phys.* **2004**, *120*, 5096−5103.

(2) Kim, Z. H.; Bechtel, H. A.; Camden, J. P.; Zare, R. N. Effect of Bending and Torsional Mode Excitation on the Reaction Cl + CH_4 → HCl + CH_3. *J. Chem. Phys.* **2005**, *122*, 084303−084307.

(3) Camden, J. P.; Bechtel, H. A.; Brown, D. J. A.; Zare, R. N. Effects of C−H Stretch Excitation on the H + CH_4 Reaction. *J. Chem. Phys.* **2005**, *123*, 134301−134309.

(4) Yoon, S.; Henton, S.; Zirkovic, A. N.; Crim, F. F. The Relative Reactivity of the Stretch-Bend Combination Vibrations of CH_4 in the Cl ($^2P_{3/2}$) + CH_4 Reaction. *J. Chem. Phys.* **2002**, *116*, 10744−10752.

(5) Yoon, S.; Holiday, R. J.; Crim, F. F. Control of Bimolecular Reactions: Bond-Selected Reaction of Vibrationally Excited CH_3D with Cl ($^2P_{3/2}$). *J. Chem. Phys.* **2003**, *119*, 4755−4761.

(6) Yoon, S.; Holiday, R. J.; Silbert, E. L., III; Crim, F. F. The Relative Reactivity of CH_3D Molecules with Excited Symmetric and Antisymmetric Stretching Vibrations. *J. Chem. Phys.* **2003**, *119*, 9568−9575.

(7) Polanyi, J. C. Concepts in Reaction Dynamics. *Acc. Chem. Res.* **1972**, *5*, 161−168.

(8) Nesbitt, D. J.; Field, R. W. Vibrational Energy Flow in Highly Excited Molecules: Role of Intramolecular Vibrational Redistribution. *J. Phys. Chem.* **1996**, *100*, 12735−12756.

(9) Smith, R. R.; Kilelea, D. R.; DelSesto, D. F.; Utz, A. L. Preference for Vibrational over Translational Energy in a Gas-Surface Reaction. *Science* **2004**, *304*, 992−995.

(10) Juurlink, L. B. F.; McCabe, P. R.; Smith, R. R.; DiCologero, C. L.; Utz, A. L. Eigenstate-Resolved Studies of Gas-Surface Reactivity: CH4 (ν_3) Dissociation on Ni(100). *Phys. Rev. Lett.* **1999**, *83*, 868−871.

(11) Higgins, J.; Conjusteau, A.; Scoles, G.; Bernasek, S. L. State Selective Vibrational ($2\nu_3$) Activation of the Chemisoption of Methane on Pt(111). *J. Chem. Phys.* **2001**, *114*, 5277−5283.

(12) Juurlink, L. B. F.; Smith, R. R.; Kilelea, D. R.; Utz, A. L. Comparative Study of C−H Stretch and Bend Vibrations in Methane Activation on Ni(100) and Ni(111). *Phys. Rev. Lett.* **2005**, *94*, 208303−208306.

(13) Maroni, P.; Papageorgopoulos, D. C.; Sacchi, M.; Dang, T. T.; Beck, R. D.; Rizzo, T. R. State-Resolved Gas-Surface Reactivity of Methane in the Symmetric C−H Stretch Vibration on Ni(100). *Phys. Rev. Lett.* **2005**, *94*, 246104−246107.
(14) Zhang, D. H.; Light, J. C. Mode Specificity in the H + HOD Reaction. Full-Dimensional Quantum Study. *J. Chem. Soc. Faraday Trans.* **1997**, *93*, 691−697.
(15) Yan, S.; Wu, Y.-T.; Zhang, B.; Yue, X.-F.; Liu, K. Do Vibrational Excitations of CHD_3 Preferentially Promote Reactivity Toward the Chlorine Atom? *Science* **2007**, *316*, 1723−1726.
(16) Espinosa-Garcia, J. Quasi-Classical Trajectory Calcualtions Analyzing the Role of Vibrational and Translational Energy in the F + CH_2D_2 Reaction. *J. Chem. Phys.* **2009**, *130*, 054305−054315.
(17) Espinosa-Garcia, J. Vibrational Versus Translational Energies in the F + CH_4 Reaction: A Comparison with the F + CH_2D_2 Reaction Using Quasi-Classical Trajectory Methods. *Chem. Phys. Lett.* **2010**, *488*, 153−157.
(18) Espinosa-Garcia, J.; Bravo, J. L.; Rangel, C. New Analytical Potential Energy Surface for the F(^{2}P) + CH_4 Hydrogen Abstraction Reaction: Kinetics and Dynamics. *J. Phys. Chem. A* **2007**, *111*, 2761−2771.
(19) Monge-Palacios, M.; Rangel, C.; Espinosa-Garcia, J. Ab Initio Based Potential Enrgy Surface and Kinetics Study of the OH + NH_3 Hydrogen Abstraction Reaction. *J. Chem. Phys.* **2013**, *138*, 084305−084318.
(20) Jeffries, J. B.; Smith, G. P. Kinetics of the Reaction Hydroxyl−Ammonia. *J. Phys. Chem.* **1986**, *90*, 487−491.
(21) Atkinson, R.; Baulch, D. L.; Cox, R. A.; Crowley, J. N.; Hampson, R. F.; Hynes, R. G.; Jenkin, M. E.; Rossi, M. J.; Troe, J. Evaluated Kinetics and Photochemical Data for Atmospheric Chemistry: Volume I. Gas Phase Reactions of Ox, HOx, NOx and SOx Species. *Atmos. Chem. Phys.* **2004**, *4*, 1461−1738.
(22) Monge-Palacios, M.; Corchado, J. C.; Espinosa-Garcia, J. Bond and Mode Selectivity in the OH + NH_3 Reaction. A Quasi-Classical Trajectory Calculation. *J. Chem. Phys.* **2013**, submitted.
(23) Butkovskaya, N. I.; Setser, D. W. Infrared Chemiluminiscence from Water-Forming Reactions: Characterization of Dynamics and Mechanisms. *Int. Rev. Phys. Chem.* **2003**, *22*, 1−72.
(24) Porter, R. N.; Raff, L. M. Classical Trajectory Methods in Molecular Collisions. In *Dynamics of Molecular Collisions*; Miller, W. H., Ed.; Plenum Press: New York, 1976; pp 1−52.
(25) Truhlar, D. G.; Muckerman, J. T. Reactive Scattering Cross Sections III: Quasiclassical and Semiclassical Methods. In *Atom−Molecules Collision Theory*; Bernstein, R. B., Ed.; Plenum Press: New York, 1979; pp 505−566.
(26) Raff, L. M.; Thompson, D. L. The Classical Trajectory Approach to Reactive Scattering. In *Theory of Chemical Reaction Dynamics*; Baer, M., Ed.; CRC Press: Boca Raton, FL, 1985; Vol. 3, pp 1−121.
(27) Hu, X.; Hase, W. L.; Pirraglia, T. Vectorization of the General Monte Carlo Classical Trajectory Program VENUS. *J. Comput. Chem.* **1991**, *12*, 1014−1024.
(28) Peslherbe, G. H.; Wang, H.; Hase, W. L. Monte Carlo Sampling for Classical Trajectory Simulations. *Adv. Chem. Phys.* **1999**, *105*, 171−201.
(29) Hase, W. L.; Duchovic, R. J.; Hu, X.; Komornicki, A.; Lim, K. F.; Lu, D.-H.; Peslherbe, G. H.; Swamy, K. N.; Van de Linde, S. R.; Varandas, A. J. C.; Wang, H.; Wolf, R. J. VENUS96: A General Chemical Dynamics Computer Program. *QCPE Bull.* **1996**, *16*, 43.
(30) See, for example, recent papers and references therein. Bonnet, L.; Rayez, J. C. Gaussian Weighting in the Quasiclasical Trajectory Method. *Chem. Phys. Lett.* **2004**, *397*, 106−109. Marques, J. M. C.; Martinez-Nuñez, E.; Fernandez-Ramos, A.; Vazquez, S. A. Trajectory Dynamics Study of the Ar + CH_4 Dissociation Reaction at High Temperatures: The Importance of the Zero-Point Energy Effects. *J. Phys. Chem. A* **2005**, *109*, 5415−5423. Duchovic, R. J.; Parker, M. A. A Quasi-Classical Trajectory Study of the Reaction H + O_2 = OH + O with the O_2 Reagent Vibrationally Excited. *J. Phys. Chem.* **2005**, *109*, 5883−5896.
(31) Varandas, A. J. C. A Novel Non-Active Model to Account for the Leak of Zero-Point Energy in Trajectory Calculations. Application to H + O_2 Reaction Near Threshold. *Chem. Phys. Lett.* **1994**, *225*, 18−27.
(32) Guo, Y.; Thomson, D. L.; Sewell, T. D. Analysis of the Zero-Point Energy Problem in Classical Trajectory Simulations. *J. Chem. Phys.* **1996**, *104*, 576−582.
(33) Bonnet, L. The Method of Gaussian Weighted Trajectories. III. An Adiabaticity Correction Proposal. *J. Chem. Phys.* **2008**, *128*, 044109−044115.
(34) Nyman, G.; Davidsson, J. A. Low-Energy Quasiclassical Trajectory Study of O(^{3}P) + OH = O_2 + H. II. Rate Constants and Recrossing, Zero-Point Energy Effects. *J. Chem. Phys.* **1990**, *92*, 2415−2422.
(35) Varandas, A. J. C. Excitation Function for H + O_2 Reaction: A Study of Zero-Point Energy Effects and Rotational Distributions in Trajectory Calculations. *J. Chem. Phys.* **1993**, *99*, 1076−1085.
(36) Corchado, J. C.; Espinosa-Garcia, J. Product Vibrational Distributions in Polyatomic Species Based on Quasiclassical Trajectory Calculations. *Phys. Chem. Chem. Phys.* **2009**, *11*, 10157−10164.
(37) Miller, W. H.; Handy, N. C.; Adams, J. E. Reaction Path Hamiltonian for Polyatomic Molecules. *J. Chem. Phys.* **1980**, *72*, 99−112.
(38) Duchovic, R.; Schatz, G. C. The FFT Method for Determining Semiclassical Eigenvalues: Application to Asymmetric Top Rigid Rotors. *J. Chem. Phys.* **1986**, *84*, 2239−2246.
(39) Schatz, G. C. A Program for Determining Primitive Semi-classical Eigenvlaues for Vibrating/Rotating Triatomic Molecules. *Comput. Phys. Commun.* **1988**, *51*, 135147.
(40) Kraka, E.; Dunning, T. H. Characterization of Molecular Potential Energy Surfaces: Critical Points, Reactions paths and Reaction Valleys. In *Advances in Molecular Electronic Structure Theory*; JAI: New York, 1990; Vol. *1*, pp 129−173.
(41) Herzberg, G. *Infrared and Raman Spectra*; D. Van Nostrand: New York, 1945.
(42) Corchado, J. C.; Chuang, Y.-Y.; Fast, P. L.; Hu, W.-P.; Liu, Y.-P.; Lynch, G. C.; Nguyen, K. A.; Jackels, C. F.; Fernandez-Ramos, A.; Ellingson, B. A.; Lynch, B. J.; Melissas, V. S.; Villà, J.; Rossi, I.; Coitiño, E. L.; Pu, J.; Albu, T. V.; Steckler, R.; Garrett, B. C.; Isaacson, A. D.; Truhlar, D. G. *Polyrate 9.5*; University of Minnesota: Minneapolis, MN, 2007.
(43) Nyman, G. Quantum Scattering Calculations on the NH_3 + OH = NH_2 + H_2O Reaction. *J. Chem. Phys.* **1996**, *104*, 6154−6168.
(44) Leitner, D. M. Influence of Quantum Energy Flow and Localization on Molecular Isomerisation in Gas and Condensed Phases. *Int. J. Quantum Chem.* **1999**, *75*, 523−529.
(45) Leitner, D. M.; Gruebele, M. A Quantum Model of Restricted Vibrational Energy Flow on the Way to the Transition State in Unimolecular Reactions. *Mol. Phys.* **2008**, *106*, 433−442.
(46) Sanson, J.; Corchado, J. C.; Rangel, C.; Espinosa-Garcia, J. Quasiclassical Trajectory Calculations Comparing the Reactivity and Dynamics of Symmetric and Asymmetric Stretch and the Role of the Bending Mode Excitations of Methane in the Cl + CH_4 Reaction. *J. Chem. Phys.* **2006**, *124*, 074312−074318.
(47) Simons, J. P. Spiers Memorial Lecture Stereochemistry and Control in Molecular Reaction Dynamics. *Faraday Discuss.* **1999**, *113*, 1−25.